TITLE PAGE

Title

Complete genome assembly of clinical multidrug resistant *Bacteroides fragilis* isolates enables comprehensive identification of antimicrobial resistance genes and plasmids.

Running title

Genomes and plasmids of six clinical MDR *B. fragilis*

Author names

Thomas V. Sydenham[1,2,3]*, Søren Overballe-Pedersen[4], Henrik Hasman[4], Hannah Wexler[5], Michael Kemp[1,2], Ulrik S. Justesen[1,2]

Affiliations

[1]Research Unit of Clinical Microbiology, Department of Clinical Research, University of Southern Denmark, Odense, Denmark; [2]Department of Clinical Microbiology, Odense University Hospital, Odense, Denmark; [3]Department of Clinical Microbiology, Lillebaelt Hospital, Vejle, Denmark; [4]Bacteria, Parasites & Fungi, Statens Serum Institut, Copenhagen, Denmark;[5] GLAVA Health Care System and David Geffen School of Medicine at UCLA, Los Angeles, CA, United States.

Corresponding author

Thomas V. Sydenham, Thomas.sydenham@rsyd.dk

ORCIDs

Thomas V. Sydenham: 0000-0003-1058-2449

Henrik Hasman: 0000-0001-6314-2709

Michael Kemp: 0000-0001-5989-0421

Ulrik S. Justesen: 0000-0002-6130-1902

KEYWORDS

Bacteroides fragilis; antimicrobial resistance; genome sequencing; plasmid; oxford nanopore; hybrid assembly; insertion sequences

REPOSITORIES

Sequence files (MinION reads de-multiplexed with Deepbinner and basecalled with Albacore in fast5 format and Illumina MiSeq reads in fastq format) and final genome assemblies have been deposited to NCBI/ENA/DDBJ under Bioproject accessions PRJNA525024, PRJNA244942, PRJNA244943, PRJNA244944, PRJNA253771, PRJNA254401, and PRJNA254455

ABSTRACT

Bacteroides fragilis constitutes a significant part of the normal human gut microbiota and can also act as an opportunistic pathogen. Antimicrobial resistance and the prevalence of antimicrobial resistance genes are increasing, and prediction of antimicrobial susceptibility based on sequence information could support targeted antimicrobial therapy in a clinical setting. Complete identification of insertion sequence (IS) elements carrying promoter sequences upstream of resistance genes is necessary for prediction of antimicrobial resistance. However, *de novo* assemblies from short reads alone are often fractured due to

repeat regions and the presence multiple copies of identical IS elements. Identification of plasmids in clinical isolates can aid in the surveillance of the dissemination of antimicrobial resistance and comprehensive sequence databases support microbiome and metagenomic studies. Here we test several short-read, hybrid and long-lead assembly pipelines by assembling the type strain *B. fragilis* CCUG4856T (=ATCC25285=NCTC9343) with Illumina short reads and long reads generated by Oxford Nanopore Technologies (ONT) MinION sequencing. Hybrid assembly with Unicycler, using quality filtered Illumina reads and Filtlong filtered and Canu corrected ONT reads produced the assembly of highest quality. This approach was then applied to six clinical multidrug resistant *B. fragilis* isolates and, with minimal manual finishing of chromosomal assemblies of three isolates, complete, circular assemblies of all isolates were produced. Eleven circular, putative plasmids were identified in the six assemblies of which only three corresponded to a known cultured *Bacteroides* plasmid. Complete IS elements could be identified upstream of antimicrobial resistance genes, however there was not complete correlation between the absence of IS elements and antimicrobial susceptibility. As our knowledge on factors that increase expression of resistance genes in the absence of IS elements is limited, further research is needed prior to implementing antimicrobial resistance prediction for *B. fragilis* from whole genome sequencing.

IMPACT STATEMENT

Bacterial whole genome sequencing is increasingly used in public health, clinical, and research laboratories for typing, identification of virulence factors, phylogenomics, outbreak investigation and identification of antimicrobial resistance genes. In some settings, diagnostic microbiome amplicon sequencing or metagenomic sequencing directly from clinical samples is already implemented and informs treatment decisions. The prospect of prediction of antimicrobial susceptibility based on resistome identification holds promises for shortening time from sample to report and informing treatment decisions. Databases with comprehensive reference sequences of high quality are a necessity for these purposes. *Bacteroides fragilis* is an important part of the human commensal gut microbiota and is also the most commonly isolated anaerobic bacterium from non-faecal clinical samples but few complete genome and plasmid assemblies are available through public databases. The fragmented assemblies from short read de novo assembly often negate the identification of insertion sequences upstream of antimicrobial resistance gens, which is necessary for prediction of antimicrobial resistance from whole genome sequencing. Here we test multiple assembly pipelines with short read Illumina data and long read data from Oxford Nanopore Technologies MinION sequencing to select an optimal pipeline for complete genome assembly of *B. fragilis*. However, *B. fragilis* is a highly plastic genome with multiple inversive repeat regions, and complete genome assembly of six clinical multidrug resistant isolates still required minor manual finishing for half the isolates. Complete identification of known insertion sequences and resistance genes was possible from the complete genome. In addition, the current catalogue of *Bacteroides* plasmid sequences is augmented by eight new plasmid sequences that do not have corresponding, complete entries in the NCBI database. This work almost doubles the number of publicly available complete, finished chromosomal and plasmid *B. fragilis* sequences paving the way for further studies on antimicrobial resistance prediction and increased quality of microbiome and metagenomic studies.

ABBREVIATIONS

AMR, antimicrobial resistance; WGS, whole genome sequencing; IS, insertion sequence; ONT, Oxford Nanopore Technologies;

DATA SUMMARY

1. Sequence read files (Oxford Nanopore (ONT) fast5 files and Illumina fastq files) as well as the final genome assemblies have been deposited to NCBI/ENA/DDBJ under Bioproject accessions PRJNA525024, PRJNA244942, PRJNA244943, PRJNA244944, PRJNA253771, PRJNA254401, and PRJNA254455.

2. Fastq format of demultiplexed ONT reads trimmed of adapters and barcode sequences are available at doi.org/10.5281/zenodo.2677927
3. Genome assemblies from the assembly pipeline validation are available at doi: doi.org/10.5281/zenodo.2648546.
4. Genome assemblies corresponding to each stage of the process of the assembly are available at doi.org/10.5281/zenodo.2661704.
5. Full commands and scripts used are available from GitHub: https://github.com/thsyd/bfassembly as well as a static version at doi.org/10.5281/zenodo.2683511

INTRODUCTION

Bacteroides fragilis is a Gram-negative anaerobic bacterium that is commensal to the human gut but can act as an opportunistic pathogen; it is the most commonly isolated anaerobic bacteria from non-faecal clinical samples (1). Antimicrobial resistance rates are increasing for *B. fragilis*, especially for carbapenems and metronidazole, two widely used antimicrobials for treatment of severe infections and anaerobe bacteria (2,3). Antimicrobial susceptibility testing of anaerobes using agar dilution or gradient strip methods can be costly and labour intensive and despite efforts to validate disk diffusion as a less expensive option, turn-around time will still be least 18 hours and validation for individual species will be required (4).

Antimicrobial resistance prediction from bacterial whole genome sequences, from cultured isolates as well as metagenomes, could be implemented in clinical microbiology in the near future, with the potential for improved sample-to-report turnover time and possibly eliminating the need for phenotypical testing for individual species (5–8). For a few species, prediction of antimicrobial resistance from WGS has been validated, but for the majority of clinical relevant species challenges still remain (6,9,10).

Based on DNA-DNA hybridisation studies, *B. fragilis* can be divided into two DNA homology groups (division I and II), whose ribosomal contents are so different that the two divisions can be distinguished by mass spectrometry routinely used to identify isolates in clinical laboratories (11). *B. fragilis* division I carry the chromosomal cephalosporinase gene *cepA* whilst *B. fragilis* division II harbour the chromosomal metallo-β-lactamase gene *cfiA* (also known as *ccrA*) (12,13). The *cfiA* gene can confer resistance to carbapenems, a class of antimicrobials usually reserved for patients with severe sepsis or infections with multidrug-resistant bacteria. But expression levels are partly controlled by insertion sequence (IS) elements carrying promotor sequences inserted upstream of the gene and only 30-50% of clinical isolates that harbour *cfiA* display phenotypically reduced susceptibility to carbapenems (3). The same pattern of expression control can be observed for genes associated with resistance to metronidazole (*nim* genes) and clindamycin (*erm* genes) (1).

In 2014 we observed that identification of IS elements upstream of known antimicrobial resistance genes in *B. fragilis* was hampered in short read *de novo* assemblies even though the genes could be identified (14). This occurred because contigs were often terminated close to the start of the resistance genes, presumably due to the proliferation of multiple copies of the same IS elements throughout the *B. fragilis* genomes. Genome assemblies from short read sequencing technologies alone most often result in fragmented assemblies because of repetitive regions and genome elements with multiple occurrences in the chromosomes and plasmids (15,16). Therefore, we could not predict antimicrobial resistance (AMR) phenotypes in *B. fragilis* using only short reads for WGS since IS element identification is a prerequisite for correct genotype-phenotype associations. Long read sequencing technologies are increasingly being utilised to increase the contiguity of bacterial genome assemblies and often result in complete, closed chromosomes and plasmids (17–20). This provides possibilities for comprehensive identification of IS elements, insights into genome structures and characterisation of other mobilisable elements and associated genes. Complete identification and characterisation of plasmids in sequenced isolates would allow for improved analysis of the plasmid-mediated spread of antimicrobial resistance.

130 Bioinformatic analysis of WGS data depends heavily on high-quality reference databases. Anaerobes make
131 up most of the bacterial human commensal microbiota but are most likely underrepresented in public
132 databases of whole genomes from cultured isolates. The NCBI Genome database (accessed 31-03-2019)
133 contains genome sequences of 191,411 bacteria of which 13,483 are marked as complete assemblies. Only
134 seven of these are *Bacteroides fragilis* (21–27). In comparison there are 776 assemblies of *E. coli* marked as
135 complete and 398 of *S. aureus*. Improving the representation of complete assemblies of *B. fragilis* in the
136 public genome databases will support the development of antimicrobial resistance prediction from WGS as
137 well as microbiome and metagenomic analysis projects.

138 The aims of this study were to select an optimal assembly software pipeline for complete, circular assembly
139 of *Bacteroides fragilis* and demonstrate the utility of complete assembly for both plasmid identification and
140 comprehensive detection of genes and IS elements associated with antimicrobial resistance. We assembled
141 the *B. fragilis* CCUG4856T (= ATCC25285 = NCTC9343) reference strain utilising long reads generated with
142 the MinION sequencer from Oxford Nanopore Technology (ONT) and high-quality Illumina short reads and
143 selected the best assembly pipeline by comparing assemblies to the Sanger sequenced reference NCTC9343
144 (RefSeq accesion GCF_000025985.1). The best assembly pipeline was then applied to six clinical multi-drug
145 resistant *B. fragilis* isolates from our 2014 study (14).

146 **METHODS**

147 **Culture conditions and DNA extraction**

148 *Bacteroides fragilis CCUG4856T* and the six strains described in our previous study were included (14,21).
149 Strains were stored at -80° in beef extract broth with 10% glycerol (SSI Diagnostica) and cultured on solid
150 chocolate agar with added vitamin K and cysteine (SSI Diagnostica) for 48 hrs in an anaerobic atmosphere
151 at 35 °C. Ten µl of culture was transferred to 14 ml saccharose serum broth (SSI Diagnostica) and incubated
152 for 18 hrs under the same conditions. DNA was then extracted using the Genomic-Tip G/500 kit (Qiagen)
153 following the manufacturers protocol for Gram negative bacteria and eluted into 5 mM Tris pH 7.5 0.5 mM
154 EDTA buffer. Quality control was performed by measuring fragment length on a TapeStation 2500
155 (Genomic DNA ScreenTape, Agilent), purity on the NanoDrop (ThermoFisher Scientific) and concentration
156 on the Qubit (dsDNA BR kit; Invitrogen). The eluted DNA was then stored at -20 °C.

157 **Illumina library preparation, sequencing and quality control**

158 The strains had previously been sequenced and assembled using Illumina short reads for our previous study
159 (14), but to minimise biological disparities we opted to re-sequence with Illumina using the same DNA
160 extraction prepared for long read sequencing. Paired-end libraries were generated using the Nextera XT
161 DNA sample preparation kit (Illumina) according to the manufacturer's protocol. DNA was sequenced on a
162 MiSeq sequencer (Illumina) with 150 bp reads for a theoretical read depth of 100x. Read quality metrics
163 were evaluated using FastQC (https://www.bioinformatics.babraham.ac.uk/projects/fastqc/) and fastp
164 v0.19.6 (28). Filterbytile from the BBmap package (http://sourceforge.net/projects/bbmap/) was used for
165 removing low-quality reads based on positional information on the sequencing flowcell and TrimGalore
166 (http://www.bioinformatics.babraham.ac.uk/projects/trim_galore/), with settings --qual 20 and --length
167 126, provided additional adapter and quality trimming. FastQ files were then randomly down-sampled to <
168 100x crude read depth using an estimated genome size of 5.3 Mb, as higher read depths tend to reduce
169 assembly quality (29).

170 **Nanopore library preparation and MinION sequencing**

171 Sequencing libraries were prepared using the Rapid Barcoding kit (SQK-RPB004; Oxford Nanopore
172 Technologies) following the manufacturers protocol (version RPB_9059_v1_revC_08Mar2018) with SPRI
173 bead clean up (AMPure XT beads; Beckman Coulter) as described. Sequencing was performed as multiplex
174 runs on a MinION connected to a Windows PC with MinKnow v1.15.1 using FLO-MIN106 R9.4 flowcells.

175 Raw fast5 files were transferred to the Computerome high performance cluster
176 (https://www.computerome.dk/) for analysis. Four sequencing runs were performed, as the first two runs
177 did not provide enough data for complete assembly of all isolates (see results section).

178 **Fast5 demultiplexing, base-calling, quality control and filtering**

179 The raw fast5 files were demultiplexed with Deepbinner v0.2.0 and base-called using Albacore v2.3.3,
180 retaining only those barcodes Deepbinner and Albacore agreed upon for minimal barcode misclassification
181 (30). Porechop v0.2.4 (https://github.com/rrwick/Porechop) with the *--discard_middle* option was used for
182 adapter and barcode trimming and read statistics were collected using NanoPlot (31). Filtlong v0.2.0
183 (https://github.com/rrwick/Filtlong) was used to filter the long reads by either removing the worst 10% or
184 by retaining 500Mbs in total, which ever option resulted in fewer reads.

185 **Assembly validation**

186 To select and validate the optimum assembly pipeline *Bacteroides fragilis* CCUG4856T was assembled using
187 a variety of well-known assemblers and polishing tools (Table 1). Each assembler was run with the Filtlong
188 filtered reads as input or the filtered reads corrected with Canu 1.8 (with standard settings,
189 corMinCoverage=0, or coroutCoverage=999). Canu was also tested with the unfiltered reads as input.
190 Hybrid assemblers used the filtered long reads and the filtered, trimmed and down-sampled Illumina reads.
191 Unicycler includes polishing with Racon and Pilon. For assemblers other than Unicycler, Racon polishing
192 with ONT reads was run for one or two rounds and Pilon was run until no changes were made or for a
193 maximum of six rounds. Racon polishing with Illumina reads was run for one round.

194 The original Sanger sequenced *Bacteroides fragilis* NCTC9343 (=CCUG4856T) (21) downloaded from NCBI
195 RefSeq (accession GCF_000025985.1) was used as reference sequence for the assembly comparisons and
196 Quast v5.0.2 was used for assembly summary statistics, indel count, and K-mer-based completion (32).
197 BUSCO v3.0.2b with the bacteroidetes_odb9 dataset, CheckM v1.0.12, and Prokka v1.13.3 were used to
198 assess gene content (33–35). Average nucleotide identity was calculated using
199 https://github.com/chjp/ANI/blob/master/ANI.pl and ALE v0.9, which uses a likelihood based approach to
200 assess the quality of different assemblies, was also used to score the assemblies (36,37). Ranking of
201 assemblies was based on number of contigs, number of circular contigs, closeness to total length compared
202 to the reference genome, number of local misassembles, number of mismatches per 100 kb, number of
203 indels per 100kb, average nucleotide identity (ANI), CheckM and BUSCO scores, and the total ALE score (a
204 higher score is better). Please see https://github.com/thsyd/bfassembly for full bioinformatics methods.

205 **Genome assembly of MDR *B. fragilis* isolates**

206 The assembly strategy deemed to produce the highest quality genome for CCUG4856T was chosen for
207 initial assembly of the six MDR *B. fragilis* isolates. Manual finishing of incomplete assemblies was
208 performed using Bandage for visualisation of assembly graphs and BLASTn searches (38). Minimap2 and
209 BWA MEM were used to map reads to the assemblies for coverage graphs (39,40). Long read assembly with
210 Flye was compared to the Unicycler assembly and used to guide and validate the manual finishing results.
211 Circlator's *fixstart* task was used to fix the start position of the manually finished genomes to be at the
212 *dnaA* gene (41).

213 The assembled genomes were submitted to NCBI GenBank and annotated with PGAP (42). ABRicate v0.8.10
214 (https://github.com/tseemann/ABRicate) (with options --minid 40 --mincov 25) was used to screen for
215 antimicrobial resistance genes with the ResFinder (database date 19-08-2018), NCBI Bacterial Antimicrobial
216 Resistance Reference Gene Database (database date 19-09-2018), and CARD (v2.0.3) databases,
217 supplemented with nucleotide sequences for the multidrug efflux-pump genes *bexA* (GenBank:
218 AB067769.1:3564..4895) and *bexB* (GenBank: AY375536.1:4599..5963) (43,44). IS elements were identified
219 using ABRicate with data from the IS-finder database (http://www-is.biotoul.fr/, Update: 2018-07-25) (45).

220 **Identification of plasmids and mobile genetic elements**

221 The PLSDB web server (https://ccb-microbe.cs.uni-saarland.de/plsdb/) (data v. 2019_03_05) contains
222 bacterial plasmid sequences retrieved from the NCBI and was used for screening and identifying putative
223 plasmids sequences (46). Only hits to accessions from cultured organisms were included. Putative plasmids
224 not identified using PLSDB, were evaluated by the read depth relative to the chromosome (higher relative
225 read depth indicates plasmid sequence) and Pfam families covering known plasmid replication domains
226 from Table 1 in reference (47) were downloaded from the Pfam database (Pfam 32.0,
227 https://pfam.xfam.org/) and used for screening putative plasmids with ABRicate.

228 **RESULTS**

229 **Sequencing data quality**

230 For Illumina data, a median of 3,465,082 reads (interquartile range [IQR]: 3,177,493-5,001,077) were
231 generated for each isolate (Supplementary Table S1)). After filtering, adapter-removal and down sampling a
232 median of 449,022,741 bases (IQR: 433,517,549-530,257,210) were available per isolate with 87-96% Q30
233 bases corresponding to calculated read depths of 75-103%. The %GC content of the reads for each isolate
234 (median 42.9%, range: 42.6-43.3%) were very consistent and within the expected range for the *Bacteroides*
235 genus (40-48%) (48) .

236 Isolates were sequenced in runs multiplexed with other isolates not included in this study. Based on initial
237 test assemblies using Unicycler without filtering or Canu correction (not shown) it was concluded that data
238 from the first ONT sequencing runs were to be supplemented by additional runs to increase the chance of
239 complete assembly of all isolates. Concatenating reads from runs, a median of 75,598 reads [IQR: 50,210-
240 112,065] with a median length of 2,938-4,393 bases were generated for each isolate (Supplementary Table
241 S1). Filtering with Filtlong and correction with Canu resulted in a median of 8,515 reads (IQR: 6,226-10,370)
242 with median lengths of 6,181-38,588 for each isolate as input for the assemblies.

243 **Selecting the optimal assembly pipeline**

244 141 assemblies of *B. fragilis* CCUG4856T were generated using the various assemblers and polishing steps
245 (Supplementary Table S2). Compared to the reference genome, Unicycler assemblies were of the highest
246 quality (**Table 2**). Unicycler, with any of the read input options, produced two circular contigs of the
247 expected lengths, and the differences between the various Unicycler assemblies were minimal (**Table 3**).
248 Assemblies with Canu corrected reads showed slightly higher genome fractions and average nucleotide
249 identities to the reference and fewer mismatches and indels, when compared to Unicycler alone. Unicycler
250 assemblies corrected with Racon using Illumina reads worsened slightly overall with 0.04-0.19 more indels
251 and 0.14-0.25 more mismatches per 100 kbp. Based on this initial evaluation, the assembly pipeline using
252 Canu corrected reads with default options was chosen (Assembly "OF.CS" in **Table 3**). This would reduce
253 the number of long reads, compared to Canu correction with corMinCoverage=0, or coroutCoverage=999,
254 and thereby lead to a faster run-time for Unicycler.

255 The hybrid Unicycler assembly of CCUG4856T with standard Canu corrected ONT reads consists of two
256 circular contigs of 5,205,133 and 36,560 bp in length. The plasmid is the same length as plasmid pBF9343
257 from the reference assembly GCF_000025985.1 and the chromosome is seven bases shorter. Alignments of
258 the Sanger sequenced assembly GCF_000025985.1 with the hybrid Unicycler assembly show an 88,045 bp
259 inversion in the hybrid assembly compared to the Sanger assembly (**Figure 1**). This inversion is present in all
260 the best assemblies, including assemblies derived from solely ONT sequences or Illumina sequences
261 (Supplementary Figure S1) as well as two additional assemblies of NCTC9343/ATCC25285 from PacBio and
262 Illumina sequences downloaded from NCBI RefSeq (Supplementary Figure S2).

263 **Complete assembly of six multidrug resistant isolates**

264 Unicycler, using filtered and trimmed Illumina reads and the Filtlong filtered and Canu corrected ONT reads
265 from the first sequencing runs, generated complete, continuous, circular assemblies for two of the six
266 isolates (BFO18 and BFO67) (**Figure 2**). For the assemblies that were not complete with sequencing data
267 from the first MinION runs, increasing the amount of ONT data resulted in fewer contigs overall, except for
268 BF067, where the additional data from the second sequencing run led to a fragmented assembly and
269 manual finishing was necessary. Performing assembly of isolate S01 without Canu correction of the ONT
270 reads from the first sequencing resulted in a closed chromosome and performing Canu correction of reads
271 resulted in a fragmentation of the chromosome. This was ameliorated by including more ONT data. By
272 manual finishing using read mapping and additional assembly with Flye, the remaining three assemblies
273 were circularised. Chromosomes varied in length from 5,141,257 – 5,504,076 bp. Alignment of ONT and
274 Illumina reads to the chromosome assemblies showed even coverage for both sequencing technologies
275 (Supplementary Figure S3). For BFO85 a >100% relative read depth increase was observed at approximately
276 25kb-38kb. This could represent a 12 kb repeat region that was not resolved in the assembly. Seven (47%)
277 of the 15 PGAP annotated CDS' in the 13kb region were annotated as hypothetical proteins. None of the
278 annotated CDS' represented mobilisable proteins.

279 **Eleven putative plasmid sequences were identified**

280 A total of 11 putative circular plasmids were identified in the six *B. fragilis* isolates (**Table 4**). Zero to three
281 putative plasmids were identified per isolate with lengths varying from 2,782 to 85,671bp.

282 The PLSDB database contains NCBI RefSeq plasmid sequences marked as complete. Three of the 11
283 putative plasmid sequences were found to match (ID > 98%) a sequence in PLSDB (**Table 4**). These three all
284 matched the cryptic plasmid pBFP35 (49). The NCBI Nucleotide database was queried using BLASTn with
285 the remaining unidentified putative plasmid sequences (50). BFO18 putative plasmid sequence pBFO18_1
286 (7,221 bp) resembles plasmid pIP421, a 7.2kb plasmid with metronidazole resistance gene *nimD* and
287 IS*1169.* Partial sequences in NCBI GenBank spanning the *nimD* gene, IS element and *RepA* (GenBank
288 Y10480.1 and X86702.1) showed 99 %ID to their alignment to pBFO18_1 (not shown) (51,52). Strain S01
289 putative plasmid sequence pBFS01_2 (8,331 bp) showed 99.87 %ID to the 1486bp partial sequence of *B.*
290 *fragilis* plasmid pBF388c (GenBank AM042593.1), a 8.3kb conjugative plasmid harbouring *nimE* and IS*Bf6*
291 (53).

292 None of the three putative plasmid sequences of strain BFO18 could be identified using the PLSDB but
293 querying the NCBI nucleotide database using BLASTn revealed hits for all three. The hits corresponded to
294 circularised sequences (%ID: 99.56-99.96, %COV: 100) assembled from mobilome metagenomic sequencing
295 of the uncultured caecum content from a rat trapped at Bispebjerg Hospital in Copenhagen, Denmark (two
296 hours' drive from Odense University Hospital where BFO18 was isolated from a patient's blood culture)
297 (Supplementary Table S3) (47,54). BLASTn searches of the remaining unidentified putative plasmids from
298 the other strains did not reveal complete hits.

299 Using ABRicate with the plasmid replication domains collected from the Pfam database, all putative
300 plasmids, except pBF017_1 and pBFS01_1, were found to have recognised replicon domains (**Table 4**). DNA
301 fragments of sizes matching pBFO17_1 and pBFS01_1 were detected by PFGE of S1 endonuclease
302 restriction enzyme treated plasmid DNA extracts (Supplementary Figure S4) and the circular structures of
303 the two sequences lacking a predicted replication domain, were confirmed manually by visually inspecting
304 BLASTn mapping of ONT sequences longer than 10 kbp to the assembled plasmid sequences with CLC
305 Genomics Workbench 10 (Qiagen). Eleven and 22 ONT reads spanned the complete lengths of pBFO17_1
306 and pBFS01_1 respectively and contained no other elements. pBFO17_1 and pBFS01_1 demonstrate a
307 degree of similarity of close to 100%, except for an approximate total of 7,500 bp transposase and
308 prophage sequences in pBF017_1 (**Figure 3**). No alignment to chromosomal sequences of any of the
309 included *B. fragilis* isolates was observed using progressiveMauve (not shown) (55).

310 The GC content of pBFO17_1 and pBFS01_1 are 36.78% and 36.04% respectively. These lie within the range
311 for the *Bacteroides* genus but differ from the expected value for *B. fragilis* (43%), which could indicate that
312 the putative plasmids do not originate from *B. fragilis* (56). After supplementing the PGAP annotations with
313 RAST annotation (57), 63% (pBFO17_1) and 59% (pBFSO1_1) of CDS' remained annotated as hypothetical
314 or as domain of unknown function. Of the annotated CDS' the majority were associated with mobilisable
315 features, plasmids and phages such as *parA* and *parB*, DNA partitioning proteins, conjugative transposon
316 proteins, transposases, DNA binding motif domain containing proteins, and reverse transcriptase protein.
317 The results above support the assembly data suggesting these two sequences are in fact plasmids.

318 **Detection of antimicrobial resistance genes and Insertion sequence elements**

319 We used ABRicate to screen assemblies for AMR genes (ResFinder, NCBI and CARD databases
320 supplemented with sequences for *bexA* and *bexB*) and IS elements (IS-finder database); several AMR genes,
321 possible homologs to known AMR genes and IS elements adjunct to the AMR genes were detected (**Table**
322 **5**). Of note, isolate BFO17 contains two homologs of the metronidazole resistance gene *nimJ* (with a 100%
323 consensus) and two isolates, S01 and BFO85, harbour two homologs of the tetracycline resistance gene
324 *tetQ*. Homologs to *bexA* and *bexB* were identified with 73.53-99.12 %ID and were all confirmed with BLASTx
325 searches against the NCBI nr database, as was done in our previous study (14). Partial hits for *ugd* was
326 observed for several isolates, but with low %ID and %COV, and possible represent identification of
327 conserved domains, but not *ugd* homologs. Increased expression of the *cfiA* metallo-beta-lactamase gene,
328 *nim*-family 5-nitroimidazole genes and *erm* genes is partly regulated through IS elements containing
329 promoter sequences. Full length IS elements could be identified upstream of 11 (79%) of 14 *cfiA*, *nim* and
330 *erm* genes and upstream of two of three *CfxA4* genes and the *OXA-347* gene identified in BFO42. The
331 described *Bacteroides fragilis* promotors TAnnTTTG (-7) and TG or TTG or TGTG (-33) (58) were searched for
332 manually, but could not be identified upstream of the two *cfiA* genes in isolates BFO67 and BFO85 or the
333 *ermB* gene in BFO85 for which no IS elements could be detected upstream (not shown).

334 **Correlation between identified genes and IS elements and phenotypical resistance**

335 As in our previous study, the *cfiA* gene was identified in the five meropenem resistant isolates (**Table 5**). All
336 the *cfiA* genes were found on the chromosomal sequences. Complete IS elements were identified upstream
337 of the *cfiA* genes in BFO17, BFO18 and S01, but not in BFO67 or BFO85. MICs for meropenem and
338 imipenem were lower for these two isolates. *Nim* genes (*-A, -D, -E* and *-J*) could be found in the four
339 metronidazole resistant isolates, all with complete IS elements upstream. Three of the *nim* genes were
340 found on putative plasmids of the respective isolates. The four clindamycin-resistant isolates all carried
341 *erm*-genes with upstream IS elements. A transposase was inserted in the *ermF-gene* in isolate BFO18,
342 splitting it in two and the same isolate demonstrated a lower clindamycin MIC (6 mg/L) than the other
343 three clindamycin resistant isolates.

344 **DISCUSSION**

345 **Hybrid genome assembly produces high quality *B. fragilis* genomes**

346 The primary aim of this study was to select and validate an assembly method to reliably complete
347 chromosome and plasmid assembly of *B. fragilis* genomes. From 141 assembly variations, a hybrid
348 approach using Filtlong filtered and Canu corrected ONT reads with quality filtered Illumina reads as input
349 to Unicycler produced a complete, closed assembly of *B. fragilis* CCUG4295T with high similarity to the
350 reference assembly of the original Sanger sequenced reference assembly. An 88kb inversion was observed
351 when comparing the two assemblies. Cerdeño-Tárraga and colleagues observed difficulties in resolving
352 certain regions of the Sanger sequenced assembly of NCTC9343 due to invertible regions with flanking
353 inverted repeat sequences (21). The observed inversion in the hybrid Unicycler assembly, could be due to
354 a) a superior assembly where the longer ONT reads have overcome the shortcomings of the shorter Sanger

355 sequences, b) an incorrect assembly by Unicycler, c) a biological difference that has occurred over time
356 between the strain stored at NCTC and CCUG, or d) a biological difference that occurred during the
357 culturing of the strain, with dominance of a clone with the inversion, prior to DNA extraction as part of this
358 study. The observations that the inversion is also present in all the best assemblies from this study and
359 assemblies from two other research institutions support the conclusions that the current hybrid Unicycler
360 assembly represents the true orientation of the 88kb sequence.

361 **Complete genome assembly of three of the six multidrug resistant isolates required manual finishing**

362 The assemblies of BFO18, S01, and BFO42 were completed by Unicycler without manual intervention, but
363 the chromosomes of BFO17, BFO67, and BFO85 could only be closed by performing manual steps. The
364 manual finishing steps are time consuming, difficult to replicate and are easily biased. In order to be
365 implemented in routine clinical laboratories, large scale, automated, complete assembly of prokaryote
366 genomes require robust methods with minimal human interaction. Genome assembly using another long-
367 read assembler, Flye, supported the results of the manual finishing for two of three isolates. Flye is better
368 at resolving repeats than miniasm, the long read assembler included in the Unicycler pipeline (59). One
369 option could be to include the long-read assembly from Flye, in place of that of miniasm, to guide bridge
370 building for the higher quality Illumina-only contigs produced in the first steps of Unicycler. To resolve
371 repeats it is often necessary to have long reads that span the repeat. In prokaryotes repeats over 10kb are
372 not unusual and they are often spanned by the ONT reads generated, even by novice researchers. But
373 repeat regions of up to 120kb and duplications of 200kb have been described in some prokaryotes
374 (17,18,60). ONT sequencing runs will routinely result in many reads that span the majority of repeats, but
375 to obtain ONT reads that span specific 120-200kb repeats in a genome of interest still requires skill and a
376 certain amount of luck. Protocols for ONT sequencing have been described that result in read lengths of
377 over 2 Mb, but this requires skilled and experienced researchers and lab technicians and demands high
378 amounts of very high quality input DNA and essentially sequencing of only one isolate per MinION flowcell
379 (61).

380 ONT read depth did not serve as an indicator of whether the Unicycler assemblies would result in closed
381 chromosomal contigs in this study. Final ONT read depth, prior to Filtlong filtering and Canu correction,
382 ranged from 23-371x, but a high read depth alone, was not an indicator of closed contigs. The three
383 assemblies BF017, BFO67, and BFO85 required manual finishing to complete the assemblies and had ONT
384 raw read depths of 99-137x. After Filtlong filtering and Canu correction the median read lengths were
385 21,932-29,893b and read length N50 was 25,765-34,815b for the three isolates (Supplementary Table S1).
386 Canu correction improved the Unicycler assembly of *B. fragilis* CCUG4856T by nearly all parameters. But
387 whilst Canu correction of the data from the first sequencing run resulted in the complete assembly of
388 BFO67, the assembly of S01 worsened slightly. Increasing the amount of ONT data for BFO67 fragmented
389 the complete chromosome. However, increasing the ONT read depth did decrease the number of contigs
390 per isolate in our study overall.

391 Defining an optimal approach for complete prokaryote genome assembly is a continuous process, as
392 sequencing technologies and assembly software develop and mature. Ring and colleagues found that Canu
393 correction prior to Unicycler hybrid assembly was superior to other hybrid assembly or long read assembly
394 approaches for assembly of *Bordetella pertussis* genomes that contain long duplicated regions (18).
395 Unicycler also performs well in other studies comparing assessing genome assemblers for bacterial genome
396 and plasmid assembly (19). De Maio and colleagues recently published a preprint comparing hybrid
397 assembly strategies for 20 *Enterobacteriaceae* isolates (20). In their dataset, simply randomly subsampling
398 ONT reads to an approximate read depth of 100x was slightly superior to applying Canu correction or
399 Filtlong filtering prior to Unicycler assembly. For 85% of isolates the expected number of circular contigs
400 were all assembled. For only one additional isolate Canu correction or Filtlong filtering resulted in the
401 assembly of the expected number of circular contigs. Manual steps, including down sampling ONT reads or

402 removing the Canu correction are options to consider, if chromosomes are not complete and circularised
403 after initial Unicycler assembly, providing ONT read depth of 100x is available.

404 We chose to benchmark a selection of widely used genome assemblers for short read, long-read and hybrid
405 bacterial genome assembly as well as polishing tools for long read assemblies, but many other options have
406 been published. Most assemblers and polishing tools were run using default parameters, and it is possible
407 that further optimisation of settings for the individual software packages might have improved assemblies
408 further than was demonstrated here. As sequencing technologies and assembly software continues to
409 improve, continued validation of pipelines is advisable. Software such as poreTally provides user friendly
410 options for benchmarking genome assembly pipelines prior to implementation (62).

411 ***Bacteroides* plasmids are not well represented in public databases**

412 A secondary aim of this study was to identify plasmids in the hybrid assemblies. Automated tools have been
413 developed and validated for identification of plasmids from genome assemblies or read data, but they are
414 dependant of collated databases of known plasmid sequences. As such, tools such as PlasmidFinder or
415 mlplasmids can be applied for plasmid identification for *Enterobacteriaceae* or *Enterococcus faecium*, but *B.*
416 *fragilis* is not supported at the time of writing (63,64). Therefore, we evaluated putative plasmid sequences
417 by sequence identity and length comparison using the PLSDB webpage, identifying plasmid replication
418 domains, and using circularisation and relative coverage as indicators that a sequence represents a plasmid
419 in a given isolate.

420 Only four of the twelve plasmid sequences from the seven isolates could be identified using the PLSDB and
421 three of these were the same plasmid, pBFP35. Two other putative plasmids, pBFO18_1 and pBFS01_2
422 were likely plasmids pBF388c and pIP421 based on the partial sequences from these plasmids and plasmid
423 length. This still leaves half of the circularised, putative plasmids unidentified. The two longer putative
424 plasmids, pBFO17_1 and pBFS01_1, displayed a high degree of similarity, a GC% out of the normal range for
425 *B. fragilis*, and a relative read depth of double the reads compared to the chromosome. Most annotated
426 CDS' were associated with mobilisable elements, but no known plasmid replication domains could be
427 identified. From the sequencing data alone, we cannot conclude that they represent true plasmids,
428 however the findings above and manual inspection of long read mapping support that inference.

429 There are only 14 complete plasmid sequences from cultured *Bacteroides* isolates in the PLSDB
430 v2019_03_05, which is based on the NCBI RefSeq database. Many other *Bacteroides* plasmids have been
431 partially described, and some are represented by partial sequences or marked as contig level in the NCBI
432 nucleotide database (65–68). Metagenomic sequencing and genome assembly projects are expanding the
433 public sequence databases and screening the NCBI nucleotide database, sequences with a high degree of
434 similarity to the putative plasmid sequences from one patient isolate (BFO18) could be found. These
435 originated from a rat caecum metagenomic plasmid sequencing project from Copenhagen, a few hours'
436 drive from Odense University Hospital. To understand and perform surveillance of the dissemination of
437 plasmids there is a need for increased submissions of high quality, annotated and phenotypically validated
438 sequences of bacterial isolates including plasmids. This study adds significantly to the number of complete
439 plasmid sequences associated with *Bacteroides.*

440 **Complete assembly allows comprehensive identification of resistance determinants in *B. fragilis***

441 We also intended to comprehensively identify resistance genes and IS elements in the hybrid genome
442 assemblies. Using ABRicate with several resistance gene databases and IS-element nucleotide sequences,
443 the findings of our previous study were confirmed and enhanced. Assemblies from Illumina sequencing
444 alone would only allow partial IS element identification (14). Now, with the complete assemblies,
445 comprehensive identification of known IS elements upstream of the relevant resistance genes could be
446 completed. In our first study we used ResFinder with the available database at that time. Now, by including

several databases, and lowering the %ID threshold, the number of genes identified increased. Additionally, for as a result of the complete genome assembly of BFO17, we could now identify two copies of *nimJ*, while only one copy was identified in the short read draft assembly of the same isolate in the previous study. Husain and colleagues identified the presence of three copies of *nimJ* in strain HMW615, when describing the *nimJ* gene (69). We confirmed this finding by running ABRicate on the HMW615 assembly as done with the isolates of this study (not shown). Interestingly, RAST annotates a third *nim* gene (nucleotide positions 1,359,590..1,360,093) in the Unicycler hybrid assembly of BFO17, and the PGAP annotation includes an additional annotation of a pyridoxamine 5'-phosphate oxidase family gene (nucleotide positions 940,032..940,505), the family that includes the *nim*-genes. It is possible that one or more novel homologs of the *nim* are present in BFO17.

IS elements could be identified upstream of most relevant resistance genes. However, in three cases no IS element was present upstream of a resistance gene, even though the isolates displayed phenotypical resistance associated with increased expression of the specific gene. Known *B. fragilis* promoter sequences could not be identified upstream of the genes “missing” upstream IS elements, however *B. fragilis* promotors are still not completely described, so it is possible there are other unknown variants.

By selecting an optimal genome assembly strategy for *B. fragilis*, supplemented with minimal manual finishing efforts, and applying this to six multidrug resistant isolates, the number of complete *B. fragilis* genomes and plasmids in the public databases has now almost doubled. The future aim of performing antimicrobial resistance prediction based solely on WGS information for *B. fragilis* demands near-complete genomes for identification of IS elements upstream of resistance genes. However, we must caution that the absence of an IS element upstream of *cfiA* does not always correlate to susceptibility to carbapenems. Future studies are needed to address this, and utilising complete genome assembly for genome wide association studies is one approach that could be pursued. Technologies that provide a single solution for real-time, high-quality sequencing of long reads will be essential for implementing near real-time diagnostics of infectious diseases and characterisation of pathogens.

AUTHOR STATEMENTS

Authors and contributors

The study was conceptualised by T.V.S. and U.S.J. Funding was secured by T.V.S., M.K., H.H. and U.S.J. Data curation and investigation was performed by T.V.S.. Formal analysis was done by T.V.S. and S.O-P.. Resources were provided by M.K., T.V.S., H.H. and U.S.J.. U.S.J, H.H. and M.K. supervised the work. T.V.S wrote the original draft and edited the manuscript. U.S.J., M.K., T.V.S., H.H., S.O-P. and H.M.W revised the manuscript.

Conflicts of interest

The authors declare that there are no conflicts of interest

Funding information

Funding supporting this work was provided from the Danish Medical Research Grant [case no. 2013-5480/912523-108] as well as internal funds from the Department of Clinical Microbiology, Odense University Hospital, Odense, Denmark. Thomas V. Sydenham’s salary as a PhD student was funded by the University of Southern Denmark and he received a travel grant from the Henrik & Emilie Ovesen Foundation.

Ethical approval

Isolates were obtained as part of routine clinical care, and details about the isolates have previously been published. No ethical approvals were required.

Acknowledgements

We are very grateful to Professor Henrik Westh, Department of Clinical Microbiology, Hvidovre Hospital, Denmark, for allowing use of their Computerome High Performance Computing cluster account for data analysis and to Mikala Wang, Dept. of Clinical Microbiology, Aarhus University hospital, for gifting us the MDR *B. fragilis* strain isolated at her department. We thank Valentina Galata, Saarland University, Saarbrücken, Germany (first author of the paper describing PLSDB) and Natalie Ring, University of Bath, Bath, United Kingdom (first author of reference (18)) for kind and helpful answers to questions via e-mail.

References

1. Wexler HM. Bacteroides: the good, the bad, and the nitty-gritty. Clin Microbiol Rev. 2007 Oct;20(4):593–621. doi: 10.1128/CMR.00008-07

2. Nagy E, Urbán E, Nord CE. Antimicrobial susceptibility of Bacteroides fragilis group isolates in Europe: 20 years of experience. Clin Microbiol Infect Off Publ Eur Soc Clin Microbiol Infect Dis. 2011 Mar;17(3):371–9. doi: 10.1111/j.1469-0691.2010.03256.x

3. Ferløv-Schwensen SA, Sydenham TV, Hansen KC, Hoegh SV, Justesen US. Prevalences of antimicrobial resistance and the cfiA resistance gene in danish bacteroides fragilis group isolates since 1973. Int J Antimicrob Agents. 2017 Jun 27; doi: 10.1016/j.ijantimicag.2017.05.007

4. Nagy E, Justesen US, Eitel Z, Urbán E. Development of EUCAST disk diffusion method for susceptibility testing of the Bacteroides fragilis group isolates. Anaerobe. 2015 Feb;31:65–71. doi: 10.1016/j.anaerobe.2014.10.008

5. Zankari E, Hasman H, Kaas RS, Seyfarth AM, Agersø Y, Lund O, et al. Genotyping using whole-genome sequencing is a realistic alternative to surveillance based on phenotypic antimicrobial susceptibility testing. J Antimicrob Chemother. 2013 Apr;68(4):771–7. doi: 10.1093/jac/dks496

6. Stoesser N, Batty EM, Eyre DW, Morgan M, Wyllie DH, Del Ojo Elias C, et al. Predicting antimicrobial susceptibilities for Escherichia coli and Klebsiella pneumoniae isolates using whole genomic sequence data. J Antimicrob Chemother [Internet]. 2013 May 30 [cited 2013 Aug 19]; doi: 10.1093/jac/dkt180

7. Boolchandani M, D'Souza AW, Dantas G. Sequencing-based methods and resources to study antimicrobial resistance. Nat Rev Genet. 2019 Mar 18;1. doi: 10.1038/s41576-019-0108-4

8. Didelot X, Bowden R, Wilson DJ, Peto TEA, Crook DW. Transforming clinical microbiology with bacterial genome sequencing. Nat Rev Genet. 2012 Sep;13(9):601–12. doi: 10.1038/nrg3226

9. Davies TJ, Stoesser N, Sheppard AE, Abuoun M, Fowler PW, Swann J, et al. Reconciling the potentially irreconcilable? Genotypic and phenotypic amoxicillin-clavulanate resistance in Escherichia coli. bioRxiv. 2019 Jan 7;511402. doi: 10.1101/511402

10. Ellington MJ, Ekelund O, Aarestrup FM, Canton R, Doumith M, Giske C, et al. The role of whole genome sequencing in antimicrobial susceptibility testing of bacteria: report from the EUCAST Subcommittee. Clin Microbiol Infect Off Publ Eur Soc Clin Microbiol Infect Dis. 2017 Jan;23(1):2–22. doi: 10.1016/j.cmi.2016.11.012

11. Nagy E, Becker S, Sóki J, Urbán E, Kostrzewa M. Differentiation of division I (cfiA-negative) and division II (cfiA-positive) Bacteroides fragilis strains by matrix-assisted laser desorption/ionization time-of-

528 flight mass spectrometry. J Med Microbiol. 2011 Nov;60(Pt 11):1584–90. doi: 10.1099/jmm.0.031336-
529 0

530 12. Rogers MB, Parker AC, Smith CJ. Cloning and characterization of the endogenous cephalosporinase
531 gene, cepA, from Bacteroides fragilis reveals a new subgroup of Ambler class A beta-lactamases.
532 Antimicrob Agents Chemother. 1993 Nov;37(11):2391–400. doi: 10.1128/AAC.37.11.2391

533 13. Rasmussen BA, Gluzman Y, Tally FP. Cloning and sequencing of the class B beta-lactamase gene (ccrA)
534 from Bacteroides fragilis TAL3636. Antimicrob Agents Chemother. 1990 Aug;34(8):1590–2.

535 14. Sydenham TV, Sóki J, Hasman H, Wang M, Justesen US, ESGAI (ESCMID Study Group on Anaerobic
536 Infections). Identification of antimicrobial resistance genes in multidrug-resistant clinical Bacteroides
537 fragilis isolates by whole genome shotgun sequencing. Anaerobe. 2015 Feb;31:59–64. doi:
538 10.1016/j.anaerobe.2014.10.009

539 15. Ricker N, Qian H, Fulthorpe RR. The limitations of draft assemblies for understanding prokaryotic
540 adaptation and evolution. Genomics. 2012 Sep;100(3):167–75. doi: 10.1016/j.ygeno.2012.06.009

541 16. Page AJ, De Silva N, Hunt M, Quail MA, Parkhill J, Harris SR, et al. Robust high-throughput prokaryote
542 de novo assembly and improvement pipeline for Illumina data. Microb Genomics [Internet]. 2016 Aug
543 25 [cited 2019 Apr 17];2(8). doi: 10.1099/mgen.0.000083

544 17. Schmid M, Frei D, Patrignani A, Schlapbach R, Frey JE, Remus-Emsermann MNP, et al. Pushing the
545 limits of de novo genome assembly for complex prokaryotic genomes harboring very long, near
546 identical repeats. Nucleic Acids Res. 2018 Sep 28;46(17):8953–65. doi: 10.1093/nar/gky726

547 18. Ring N, Abrahams JS, Jain M, Olsen H, Preston A, Bagby S. Resolving the complex Bordetella pertussis
548 genome using barcoded nanopore sequencing. Microb Genomics. 2018 Nov 21; doi:
549 10.1099/mgen.0.000234

550 19. Wick RR, Judd LM, Gorrie CL, Holt KE. Completing bacterial genome assemblies with multiplex MinION
551 sequencing. Microb Genomics [Internet]. 2017 [cited 2018 Apr 3];3(10). doi: 10.1099/mgen.0.000132

552 20. Maio ND, Shaw LP, Hubbard A, George S, Sanderson N, Swann J, et al. Comparison of long-read
553 sequencing technologies in the hybrid assembly of complex bacterial genomes. bioRxiv. 2019 Jan
554 28;530824. doi: 10.1101/530824

555 21. Cerdeño-Tárraga AM, Patrick S, Crossman LC, Blakely G, Abratt V, Lennard N, et al. Extensive DNA
556 inversions in the B. fragilis genome control variable gene expression. Science. 2005 Mar
557 4;307(5714):1463–5. doi: 10.1126/science.1107008

558 22. Kuwahara T, Yamashita A, Hirakawa H, Nakayama H, Toh H, Okada N, et al. Genomic analysis of
559 Bacteroides fragilis reveals extensive DNA inversions regulating cell surface adaptation. Proc Natl
560 Acad Sci U S A. 2004 Oct 12;101(41):14919–24. doi: 10.1073/pnas.0404172101

561 23. Patrick S, Blakely GW, Houston S, Moore J, Abratt VR, Bertalan M, et al. Twenty-eight divergent
562 polysaccharide loci specifying within- and amongst-strain capsule diversity in three strains of
563 Bacteroides fragilis. Microbiology. 2010 Nov;156(Pt 11):3255–69. doi: 10.1099/mic.0.042978-0

564 24. Nikitina AS, Kharlampieva DD, Babenko VV, Shirokov DA, Vakhitova MT, Manolov AI, et al. Complete
565 Genome Sequence of an Enterotoxigenic Bacteroides fragilis Clinical Isolate. Genome Announc
566 [Internet]. 2015 May 7;3(3). doi: 10.1128/genomeA.00450-15

567 25. Risse J, Thomson M, Patrick S, Blakely G, Koutsovoulos G, Blaxter M, et al. A single chromosome
568 assembly of Bacteroides fragilis strain BE1 from Illumina and MinION nanopore sequencing data.
569 GigaScience [Internet]. 2015 Dec 4 [cited 2017 Jun 22];4. doi: 10.1186/s13742-015-0101-6

570 26. Soki, Jozsef. Bacteroides fragilis S14 genome sequencing and assembly (Data accessed on NCBI RefSeq
571 database accession GCF_001682215.1). 2015.

572 27. Ho P-L, Yau C-Y, Wang Y, Chow K-H. Determination of the mutant–prevention concentration of
573 imipenem for the two imipenem–susceptible Bacteroides fragilis strains, Q1F2 (cfiA-positive) and
574 ATCC 25282 (cfiA-negative). Int J Antimicrob Agents. 2018 Feb 1;51(2):270–1. doi:
575 10.1016/j.ijantimicag.2017.08.004

576 28. Chen S, Zhou Y, Chen Y, Gu J. fastp: an ultra-fast all-in-one FASTQ preprocessor. Bioinformatics. 2018
577 Sep 1;34(17):i884–90. doi: 10.1093/bioinformatics/bty560

578 29. Desai A, Marwah VS, Yadav A, Jha V, Dhaygude K, Bangar U, et al. Identification of Optimum
579 Sequencing Depth Especially for De Novo Genome Assembly of Small Genomes Using Next Generation
580 Sequencing Data. PLoS ONE [Internet]. 2013 Apr 12 [cited 2014 May 22];8(4). doi:
581 10.1371/journal.pone.0060204

582 30. Wick RR, Judd LM, Holt KE. Deepbinner: Demultiplexing barcoded Oxford Nanopore reads with deep
583 convolutional neural networks. bioRxiv. 2018 Sep 14;366526. doi: 10.1101/366526

584 31. De Coster W, D'Hert S, Schultz DT, Cruts M, Van Broeckhoven C. NanoPack: visualizing and processing
585 long-read sequencing data. Bioinformatics. 2018 Aug 1;34(15):2666–9. doi:
586 10.1093/bioinformatics/bty149

587 32. Gurevich A, Saveliev V, Vyahhi N, Tesler G. QUAST: quality assessment tool for genome assemblies.
588 Bioinformatics. 2013 Apr 15;29(8):1072–5. doi: 10.1093/bioinformatics/btt086

589 33. Parks DH, Imelfort M, Skennerton CT, Hugenholtz P, Tyson GW. CheckM: assessing the quality of
590 microbial genomes recovered from isolates, single cells, and metagenomes. Genome Res. 2015 Jul
591 1;25(7):1043–55. doi: 10.1101/gr.186072.114

592 34. Waterhouse RM, Seppey M, Simão FA, Manni M, Ioannidis P, Klioutchnikov G, et al. BUSCO
593 Applications from Quality Assessments to Gene Prediction and Phylogenomics. Mol Biol Evol. 2018
594 Mar 1;35(3):543–8. doi: 10.1093/molbev/msx319

595 35. Seemann T. Prokka: rapid prokaryotic genome annotation. Bioinformatics. 2014 Jul 15;30(14):2068–9.
596 doi: 10.1093/bioinformatics/btu153

597 36. Richter M, Rosselló-Móra R. Shifting the genomic gold standard for the prokaryotic species definition.
598 Proc Natl Acad Sci. 2009 Oct 22;pnas.0906412106. doi: 10.1073/pnas.0906412106

599 37. Clark SC, Egan R, Frazier PI, Wang Z. ALE: a generic assembly likelihood evaluation framework for
600 assessing the accuracy of genome and metagenome assemblies. Bioinformatics. 2013 Feb
601 15;29(4):435–43. doi: 10.1093/bioinformatics/bts723

602 38. Wick RR, Schultz MB, Zobel J, Holt KE. Bandage: interactive visualization of de novo genome
603 assemblies. Bioinforma Oxf Engl. 2015 Oct 15;31(20):3350–2. doi: 10.1093/bioinformatics/btv383

604 39. Li H. Minimap2: pairwise alignment for nucleotide sequences. Bioinformatics. 2018 Sep
605 15;34(18):3094–100. doi: 10.1093/bioinformatics/bty191

606 40. Li H, Durbin R. Fast and accurate short read alignment with Burrows-Wheeler transform. Bioinforma
607 Oxf Engl. 2009 Jul 15;25(14):1754–60. doi: 10.1093/bioinformatics/btp324

608 41. Hunt M, Silva ND, Otto TD, Parkhill J, Keane JA, Harris SR. Circlator: automated circularization of
609 genome assemblies using long sequencing reads. Genome Biol. 2015 Dec 29;16:294. doi:
610 10.1186/s13059-015-0849-0

611 42. Tatusova T, DiCuccio M, Badretdin A, Chetvernin V, Nawrocki EP, Zaslavsky L, et al. NCBI prokaryotic
612 genome annotation pipeline. Nucleic Acids Res. 2016 19;44(14):6614–24. doi: 10.1093/nar/gkw569

613 43. Zankari E, Hasman H, Cosentino S, Vestergaard M, Rasmussen S, Lund O, et al. Identification of
614 acquired antimicrobial resistance genes. J Antimicrob Chemother. 2012 Nov;67(11):2640–4. doi:
615 10.1093/jac/dks261

616 44. Jia B, Raphenya AR, Alcock B, Waglechner N, Guo P, Tsang KK, et al. CARD 2017: expansion and model-
617 centric curation of the comprehensive antibiotic resistance database. Nucleic Acids Res. 2017
618 04;45(D1):D566–73. doi: 10.1093/nar/gkw1004

619 45. Siguier P, Perochon J, Lestrade L, Mahillon J, Chandler M. ISfinder: the reference centre for bacterial
620 insertion sequences. Nucleic Acids Res. 2006 Jan 1;34(Database issue):D32-36. doi:
621 10.1093/nar/gkj014

622 46. Galata V, Fehlmann T, Backes C, Keller A. PLSDB: a resource of complete bacterial plasmids. Nucleic
623 Acids Res. 2019 Jan 8;47(D1):D195–202. doi: 10.1093/nar/gky1050

624 47. Jørgensen TS, Xu Z, Hansen MA, Sørensen SJ, Hansen LH. Hundreds of Circular Novel Plasmids and
625 DNA Elements Identified in a Rat Cecum Metamobilome. PLoS ONE [Internet]. 2014 Feb 4 [cited 2019
626 Mar 12];9(2). doi: 10.1371/journal.pone.0087924

627 48. Shah HN. The Genus Bacteroides and Related Taxa. In: Balows A, Trüper HG, Dworkin M, Harder W,
628 Schleifer K-H, editors. The Prokaryotes: A Handbook on the Biology of Bacteria: Ecophysiology,
629 Isolation, Identification, Applications [Internet]. New York, NY: Springer New York; 1992 [cited 2019
630 Mar 21]. p. 3593–607. doi: 10.1007/978-1-4757-2191-1_34

631 49. Sóki J, Wareham DW, Rátkai C, Aduse-Opoku J, Urbán E, Nagy E. Prevalence, nucleotide sequence and
632 expression studies of two proteins of a 5.6kb, class III, Bacteroides plasmid frequently found in clinical
633 isolates from European countries. Plasmid. 2010 Mar;63(2):86–97. doi:
634 10.1016/j.plasmid.2009.12.002

635 50. Database resources of the National Center for Biotechnology Information. Nucleic Acids Res. 2016 Jan
636 4;44(Database issue):D7–19. doi: 10.1093/nar/gkv1290

637 51. Trinh S, Haggoud A, Reysset G, Sebald M. Plasmids pIP419 and pIP421 from Bacteroides: 5-
638 nitroimidazole resistance genes and their upstream insertion sequence elements. Microbiol Read
639 Engl. 1995 Apr;141 (Pt 4):927–35. doi: 10.1099/13500872-141-4-927

640 52. Haggoud A, Trinh S, Moumni M, Reysset G. Genetic analysis of the minimal replicon of plasmid pIP417
641 and comparison with the other encoding 5-nitroimidazole resistance plasmids from Bacteroides spp.
642 Plasmid. 1995 Sep;34(2):132–43. doi: 10.1006/plas.1995.9994

643 53. Sóki J, Gal M, Brazier JS, Rotimi VO, Urbán E, Nagy E, et al. Molecular investigation of genetic
644 elements contributing to metronidazole resistance in Bacteroides strains. J Antimicrob Chemother.
645 2006 Feb;57(2):212–20. doi: 10.1093/jac/dki443

646 54. Hartmeyer GN, Sóki J, Nagy E, Justesen US. Multidrug-resistant Bacteroides fragilis group on the rise
647 in Europe? J Med Microbiol. 2012 Dec;61(Pt 12):1784–8. doi: 10.1099/jmm.0.049825-0

648 55. Darling AE, Mau B, Perna NT. progressiveMauve: Multiple Genome Alignment with Gene Gain, Loss
649 and Rearrangement. PLOS ONE. 2010 Jun 25;5(6):e11147. doi: 10.1371/journal.pone.0011147

650 56. Nishida H. Comparative Analyses of Base Compositions, DNA Sizes, and Dinucleotide Frequency
651 Profiles in Archaeal and Bacterial Chromosomes and Plasmids [Internet]. International Journal of
652 Evolutionary Biology. 2012 [cited 2019 Apr 26]. doi: 10.1155/2012/342482

653 57. Brettin T, Davis JJ, Disz T, Edwards RA, Gerdes S, Olsen GJ, et al. RASTtk: a modular and extensible
654 implementation of the RAST algorithm for building custom annotation pipelines and annotating
655 batches of genomes. Sci Rep. 2015 Feb 10;5:8365. doi: 10.1038/srep08365

656 58. Bayley DP, Rocha ER, Smith CJ. Analysis of cepA and other Bacteroides fragilis genes reveals a unique
657 promoter structure. FEMS Microbiol Lett. 2000 Dec 1;193(1):149–54. doi: 10.1111/j.1574-
658 6968.2000.tb09417.x

659 59. Lin Y, Yuan J, Kolmogorov M, Shen MW, Chaisson M, Pevzner PA. Assembly of long error-prone reads
660 using de Bruijn graphs. Proc Natl Acad Sci. 2016 Dec 27;113(52):E8396–405. doi:
661 10.1073/pnas.1604560113

662 60. Kamath GM, Shomorony I, Xia F, Courtade TA, Tse DN. HINGE: long-read assembly achieves optimal
663 repeat resolution. Genome Res. 2017;27(5):747–56. doi: 10.1101/gr.216465.116

664 61. Payne A, Holmes N, Rakyan V, Loose M. Whale watching with BulkVis: A graphical viewer for Oxford
665 Nanopore bulk fast5 files. bioRxiv. 2018 May 3;312256. doi: 10.1101/312256

666 62. de Lannoy C, Risse J, de Ridder D. poreTally: run and publish de novo nanopore assembler
667 benchmarks. Bioinformatics [Internet]. [cited 2019 Apr 26]; doi: 10.1093/bioinformatics/bty1045

668 63. Carattoli A, Zankari E, García-Fernández A, Larsen MV, Lund O, Villa L, et al. In Silico Detection and
669 Typing of Plasmids using PlasmidFinder and Plasmid Multilocus Sequence Typing. Antimicrob Agents
670 Chemother. 2014 Jul 1;58(7):3895–903. doi: 10.1128/AAC.02412-14

671 64. Arredondo-Alonso S, Rogers MRC, Braat JC, Verschuuren TD, Top J, Corander J, et al. mlplasmids: a
672 user-friendly tool to predict plasmid- and chromosome-derived sequences for single species. Microb
673 Genomics [Internet]. 2018 [cited 2019 May 9];4(11). doi: 10.1099/mgen.0.000224

674 65. Nguyen M, Vedantam G. Mobile genetic elements in the genus Bacteroides, and their mechanism(s)
675 of dissemination. Mob Genet Elem. 2011;1(3):187–96. doi: 10.4161/mge.1.3.18448

676 66. Shkoporov AN, Khokhlova EV, Kulagina EV, Smeianov VV, Kuchmiy AA, Kafarskaya LI, et al. Analysis of
677 a novel 8.9kb cryptic plasmid from Bacteroides uniformis, its long-term stability and spread within
678 human microbiota. Plasmid. 2013 Mar 1;69(2):146–59. doi: 10.1016/j.plasmid.2012.11.002

679 67. McNulty NP, Wu M, Erickson AR, Pan C, Erickson BK, Martens EC, et al. Effects of diet on resource
680 utilization by a model human gut microbiota containing Bacteroides cellulosilyticus WH2, a symbiont
681 with an extensive glycobiome. PLoS Biol. 2013;11(8):e1001637. doi: 10.1371/journal.pbio.1001637

682 68. Pierce JV, Bernstein HD. Genomic Diversity of Enterotoxigenic Strains of Bacteroides fragilis. PLoS ONE
683 [Internet]. 2016 Jun 27 [cited 2019 Mar 26];11(6). doi: 10.1371/journal.pone.0158171

684 69. Husain F, Veeranagouda Y, Hsi J, Meggersee R, Abratt V, Wexler HM. Two multidrug-resistant clinical
685 isolates of Bacteroides fragilis carry a novel metronidazole resistance nim gene (nimJ). Antimicrob
686 Agents Chemother. 2013 Aug;57(8):3767–74. doi: 10.1128/AAC.00386-13

687 70. Ruan J, Li H. Fast and accurate long-read assembly with wtdbg2. bioRxiv. 2019 Jan 26;530972. doi:
688 10.1101/530972

689 71. Li H. Minimap and miniasm: fast mapping and de novo assembly for noisy long sequences.
690 Bioinformatics. 2016 Jul 15;32(14):2103–10. doi: 10.1093/bioinformatics/btw152

691 72. Kolmogorov M, Yuan J, Lin Y, Pevzner PA. Assembly of long, error-prone reads using repeat graphs.
692 Nat Biotechnol. 2019 Apr 1;1. doi: 10.1038/s41587-019-0072-8

693 73. Koren S, Walenz BP, Berlin K, Miller JR, Bergman NH, Phillippy AM. Canu: scalable and accurate long-
694 read assembly via adaptive k-mer weighting and repeat separation. Genome Res. 2017 May
695 1;27(5):722–36. doi: 10.1101/gr.215087.116

696 74. Bankevich A, Nurk S, Antipov D, Gurevich AA, Dvorkin M, Kulikov AS, et al. SPAdes: A New Genome
697 Assembly Algorithm and Its Applications to Single-Cell Sequencing. J Comput Biol. 2012
698 May;19(5):455–77. doi: 10.1089/cmb.2012.0021

699 75. Antipov D, Korobeynikov A, McLean JS, Pevzner PA. hybridSPAdes: an algorithm for hybrid assembly
700 of short and long reads. Bioinformatics. 2016 Apr 1;32(7):1009–15. doi:
701 10.1093/bioinformatics/btv688

702 76. Souvorov A, Agarwala R, Lipman DJ. SKESA: strategic k-mer extension for scrupulous assemblies.
703 Genome Biol. 2018 Oct 4;19(1):153. doi: 10.1186/s13059-018-1540-z

704 77. Wick RR, Judd LM, Gorrie CL, Holt KE. Unicycler: Resolving bacterial genome assemblies from short
705 and long sequencing reads. PLOS Comput Biol. 2017 Aug 6;13(6):e1005595. doi:
706 10.1371/journal.pcbi.1005595

707 78. Loman NJ, Quick J, Simpson JT. A complete bacterial genome assembled *de novo* using only nanopore
708 sequencing data. Nat Methods. 2015 Aug;12(8):733–5. doi: 10.1038/nmeth.3444

709 79. Vaser R, Sovic I, Nagarajan N, Sikic M. Fast and accurate de novo genome assembly from long
710 uncorrected reads. Genome Res. 2017 Jan 18;gr.214270.116. doi: 10.1101/gr.214270.116

711 80. Walker BJ, Abeel T, Shea T, Priest M, Abouelliel A, Sakthikumar S, et al. Pilon: An Integrated Tool for
712 Comprehensive Microbial Variant Detection and Genome Assembly Improvement. PLOS ONE. 2014
713 Nov 19;9(11):e112963. doi: 10.1371/journal.pone.0112963

714 81. Krumsiek J, Arnold R, Rattei T. Gepard: a rapid and sensitive tool for creating dotplots on genome
715 scale. Bioinforma Oxf Engl. 2007 Apr 15;23(8):1026–8. doi: 10.1093/bioinformatics/btm039

716 82. Sullivan MJ, Petty NK, Beatson SA. Easyfig: a genome comparison visualizer. Bioinformatics. 2011 Apr
717 1;27(7):1009–10. doi: 10.1093/bioinformatics/btr039

718 83. Arndt D, Grant JR, Marcu A, Sajed T, Pon A, Liang Y, et al. PHASTER: a better, faster version of the
719 PHAST phage search tool. Nucleic Acids Res. 2016 08;44(W1):W16-21. doi: 10.1093/nar/gkw387

720

721 **TABLES AND FIGURES**

722

Genome assembler and version	Link	Reference
Wtdbg2 v2.3	https://github.com/ruanjue/wtdbg2	(70)
Miniasm v0.3r179	https://github.com/lh3/miniasm	(39,71)
Flye v2.3.7	https://github.com/fenderglass/Flye	(59,72)
Canu v1.8	https://github.com/marbl/canu	(73)
Spades (including Hybridspades) v3.13.0	https://github.com/ablab/spades	(74,75)
Skesa v2.3.0	https://github.com/ncbi/SKESA	(76)
Unicycler v0.4.7	https://github.com/rrwick/Unicycler	(77)
Assembly polishing tools		
Nanopolish v0.10.2	https://github.com/jts/nanopolish	(78)
Racon v1.3.1	https://github.com/isovic/racon	(79)
Pilon v1.22	https://github.com/broadinstitute/pilon	(80)

723 Table 1.Genome assemblers and polishing tools tested

724

Assembly	Contigs	Largest contig	Total length	Mis-assemblies	Genome fraction (%)	Mismatches per 100 kbp	Indels per 100 kbp	Average nucleotide identity	CheckM Completeness	BUSCOs: complete and single-copy/ complete and duplicate/ fragment (of 443)	Prokka genes	Prokka rRNA	Prokka tRNA	Total ALE score
GCF_000025985.1	2	5,205,140	5,241,700	0	100.000	0	0	100.0000	99.26	442/0/1	4439	19	73	-17071758.95
Skesa	46	553,341	5,201,945	3	99.237	0.23	0.15	99.9980	99.26	440/2/1	4391	2	62	-20926329.69
Spades	23	1,779,941	5,212,217	4	99.396	0.44	0.17	99.9866	99.26	440/2/1	4407	3	56	-19676529.39
Canu.OF.CO.RO2.RI.PI3	2	5,247,938	5,350,432	8	99.972	4.94	15.9	99.9752	99.26	442/0/1	4634	19	73	-19283611.73
Flye.OF.CS.PI5.RI	5	2,282,650	5,269,269	4	99.917	1.07	6.24	99.9781	99.26	441/1/1	4476	19	73	-18222322.23
Miniasm.OF.CM.RO2.PI5	3	5,204,445	5,277,434	2	99.972	5.21	17.75	99.9691	98.88	442/0/1	4607	19	73	-17789234.97
Wtdbg2.OF.CO.RO2.PI6.RI	3	5,192,352	5,234,448	7	99.723	3.23	3.04	99.9807	99.26	442/0/1	4437	19	73	-18750266.21
SpadesHybrid.CS	5	3,093,122	5,242,724	7	99.987	1.89	0.53	99.9856	99.26	440/2/1	4441	19	73	-18535980.68
Unicycler.OF.CS	2	5,205,133	5,241,693	2	99.972	0.84	0.48	99.9997	99.26	442/0/1	4435	19	73	-17200232.52

725 Table 2. Selected quality indicators for the best genome assembly of *B. fragilis* CCUG4856T per assembly pipeline. RefSeq accession GCF_000025985.1
726 was used as reference. OF: ONT reads filtered with Filtlong, CS: Canu corrected standard settings, CM: Canu corrected with option corMinCoverage=0,
727 CO: Canu corrected with option coroutCoverage=999, RO2: Two rounds of Racon polishing with ONT reads, RI: Racon polishing with Illumina reads,
728 PI[n]: Pilon polishing with Illumina reads, [n] rounds. Full results are available in Supplementary Table S2.

729

Assembly	Total length (bp)	Largest contig (bp)	Local mis-assemblies	Genome fraction (%)	Mismatches per 100 kbp	Indels per 100 kbp	K-mer-based compl. (%)	K-mer-based misjoins	Average nucletide identity	Prokka CDS	Prokka genes	Total ALE score
GCF_000025985.1	5,241,700	5,205,140	0	100.000	0	0	100.00	0	100.00000	4346	4439	-17071758.95
OF	5,241,602	5,205,042	3	99.970	1.11	0.65	99.96	0	99.99896	4343	4436	-17245134.52
OF.RI	5,241,606	5,205,046	3	99.970	1.09	0.67	99.96	3	99.99887	4345	4438	-17247815.86
OF.CS	5,241,693	5,205,133	2	99.972	0.84	0.48	99.97	1	99.99974	4342	4435	-17200232.52
OF.CS.RI	5,241,698	5,205,138	2	99.972	0.88	0.52	99.96	1	99.99968	4346	4439	-17206271.66
OF.CM	5,241,691	5,205,131	2	99.972	0.88	0.5	99.96	1	99.99966	4343	4436	-17201292.44
OF.CM.RI	5,241,696	5,205,136	2	99.972	0.95	0.55	99.97	1	99.99975	4343	4436	-17193184.79
OF.CO	5,241,693	5,205,133	2	99.972	0.84	0.48	99.97	1	99.99974	4342	4435	-17200232.52
OF.CO.RI	5,241,698	5,205,138	2	99.972	0.88	0.52	99.96	1	99.99968	4346	4439	-17206271.66

Table 3. Hybrid Unicycler assemblies of *B. fragilis* CCUG4856T. RefSeq accession GCF_000025985.1 was used as reference. OF: ONT reads filtered with Filtlong; CS: Canu corrected standard settings; CM: Canu corrected with option corMinCoverage=0; CO: Canu corrected with option coroutCoverage=999; RI: Racon polishing with Illumina reads. Unicycler performs assembly polishing with Racon (ONT reads) and Pilon. Full results are available in Supplementary Table S2.

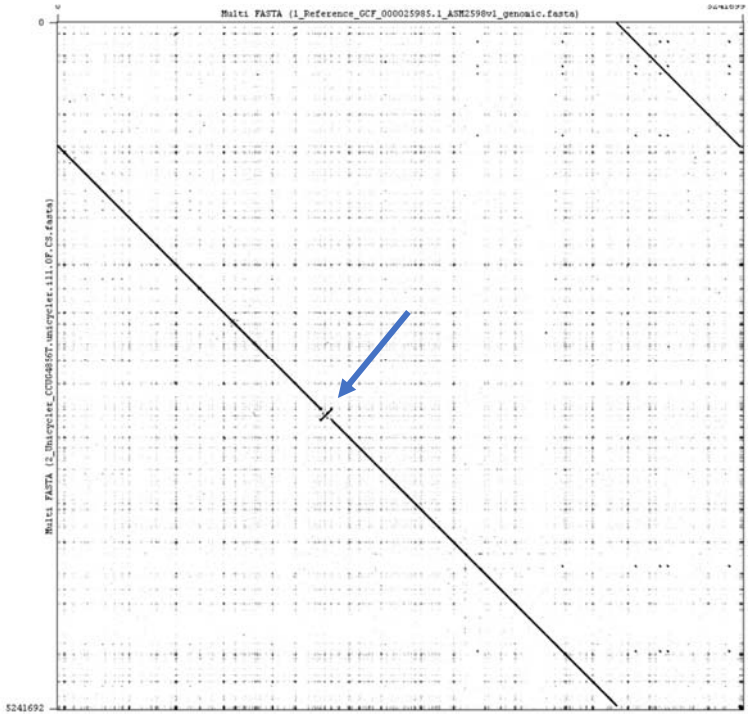

Figure 1. Dot plot matrix of the alignment of the reference assembly and the hybrid Unicycler assembly using Gepard v1.40 (81). The *B. fragilis* NCTC9343 (RefSeq GCF_000025985.1) reference assembly derived from Sanger sequencing is on the x-axis and the hybrid Unicycler assembly on the y-axis. On this otherwise near perfect alignment with high similarity, an 88,045 bp inversion with 100% ID is observed at nucleotide positions 2,941,962..3,030,006 on the Unicycler assembly (2,005,742..2,093,786 on the reference sequence) (indicated by the blue arrow).

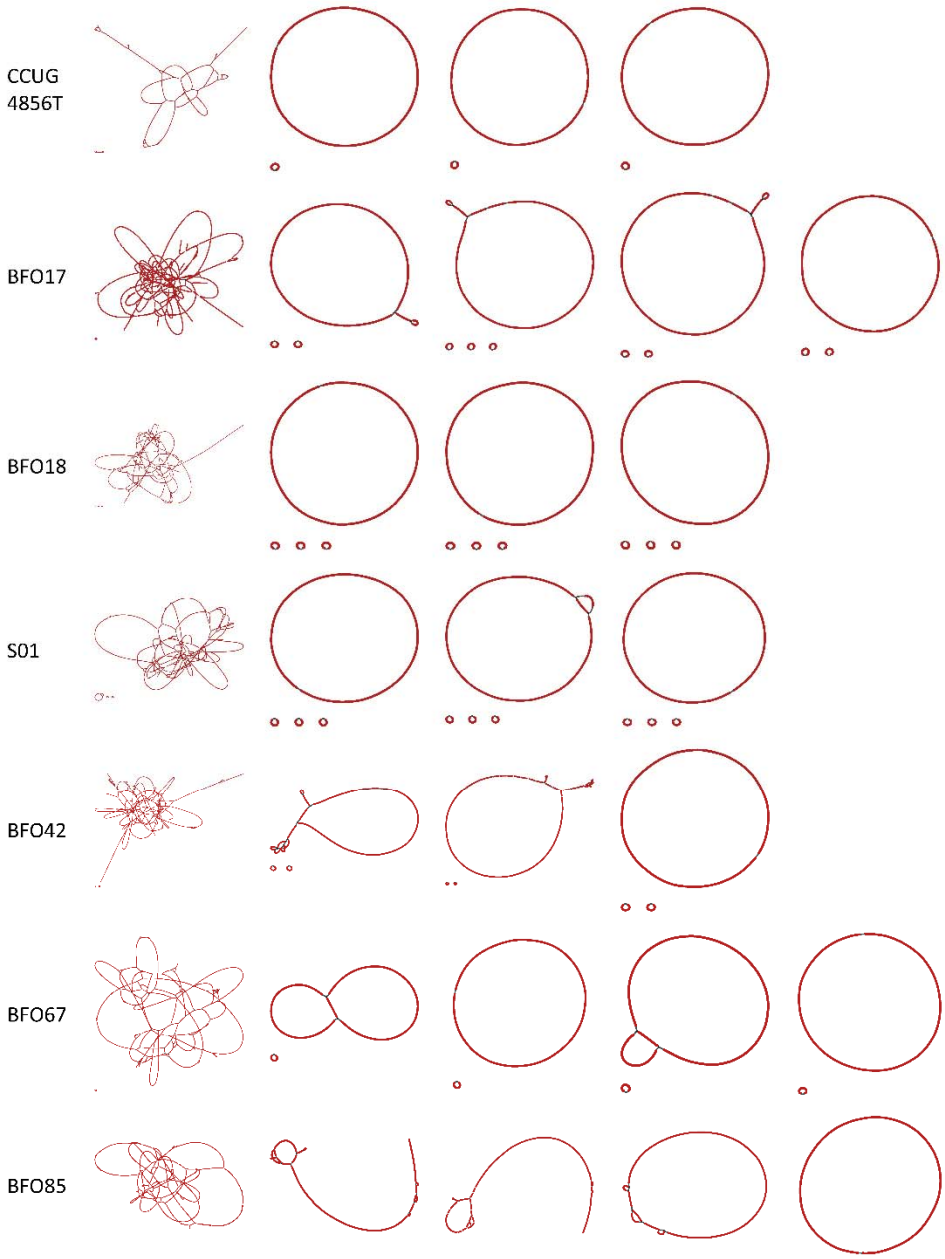

Final assemblies contig statistics		
No.	Length	Relative read depth
1	5,205,133	1.00x
2	36,560	7.42x
1	5,474,541	1.00x
2	85,671	1.85x
3	5,594	23.03x
1	5,302,644	1.00x
2	7,221	25.98x
3	4,137	50.80x
4	2,782	59.91x
1	5,325,251	1.00x
2	78,085	2.29x
3	8,331	20.99x
4	5,595	22.67x
1	5,141,257	1.00x
2	8,306	40.06x
3	5,594	40.15x
1	5,478,614	1.00x
2	6,129	94.15x
1	5,504,076	1.00x

Figure 2. Evolution of genome assemblies with added data and manual finishing. The best SPAdes assembly graphs by Unicycler with short reads only are shown on the far left. Supplying ONT reads improved the assemblies overall, but only three were circularised with singular chromosome contigs with data from the initial MinION sequencing runs. Adding additional ONT data and correcting reads with Canu did not improve assemblies for all isolates. Manual finishing was necessary to finish assemblies for three isolates. Assembly graph images generated with Bandage. Read information can be found in Supplementary Table S1.

Strain	Sequence	Length (bp)	Relative read depth	GC%	PLSDB results				Plasmid replicon family (%COV, %ID)
					Best hit accession no.	Plasmid hit name	%ID	Length of the sequence of best hit (bp)	
CCUG4856T	Chr.	5,205,133	1.00x	43.19		-	-	-	-
	pBF9343	36,560	7.42x	32.19	NC_006873.1	pBF9343	100	36,560	Rep_3 (100/100)
BFO17	Chr.	5,474,541	1.00x	43.51	-	-	-	-	-
	pBFO17_1	85,671	1.85x	36.78	NC_006873.1	pBF9343	80.7	36,560	none
	pBFO17_2	5,594	23.03x	39.65	NC_011073.1	pBFP35	99.9	5,594	Rep_1 (100/100)
BFO18	Chr.	5,302,644	1.00x	43.34	-	-	-	-	-
	pBFO18_1	7,221	25.98x	42.32	NC_015168.1	pBACSA02	85.6	19,280	Rep_3 (99.69/99.69)
	pBFO18_2	4,137	50.80x	45.40	NC_019534.1	pBFUK1	92.2	12,817	Rep_3 (100.00/98.24)
	pBFO18_3	2,782	59.91x	41.45	NC_005026.1	pBI143	94.6	2,747	RepL (89.66/49.22)[a]
S01	Chr.	5,325,251	1.00x	43.57	-	-	-	-	-
	pBFS01_1	78,085	2.29x	36.04	NC_006873.1	pBF9343	80.7	36,560	none
	pBFS01_2	8,331	20.99x	41.17	NC_015166.1	pBACSA03	95.6	6,277	Rep_3 (100.00/97.85)
	pBFS01_3	5,595	22.67x	39.62	NC_011073.1	pBFP35	99.9	5,594	Rep_1 (100.00/99.48)
BFO42	Chr.	5,141,257	1.00x	43.35	-	-	-	-	-
	pBFO32_1	8,306	40.06x	43.34	KJ830768.1	pBF69566b	96.0	11,019	RHH_1 (92.94/64.63) Rep_3 (93.64/68.31)
	pBFO32_2	5,594	40.15x	39.63	NC_011073.1	pBFP35	99.9	5,594	Rep_1 (100.00 /99.48)
BFO67	Chr.	5,478,614	1.00x	43.85	-	-	-	-	-
	pBFO67_1	6,129	94.15x	41.67	NC_011073.1	pBFP35	76.9	5,594	Rep_3 (100.00/99.69)
BFO85	Chr.	5,504,076	1.00x	43.60	-	-	-	-	-

Table 4. Putative plasmid sequences of the complete *B. fragilis* assemblies. Putative plasmid sequences from the hybrid assemblies of *B. fragilis* CCUG4856T and the six MDR *B. fragilis* isolates were screened using the PLSDB. The best hit to plasmids from cultured isolates is shown. Only three putative plasmids from the MDR *B. fragilis* isolate assemblies could be identified with confident %ID. For most sequences, plasmid replication family proteins were identified in the putative plasmids using ABRicate with a database of sequences downloaded from the Pfam database, strengthening

755 the interpretation that the circularised putative plasmid sequences do in fact represent plasmids harboured by the isolates. Notes: [a]Annotated as
756 RepA protein in the PGAP annotation. Abbreviations: %ID, %COV, no.; number, Chr.; chromosome.

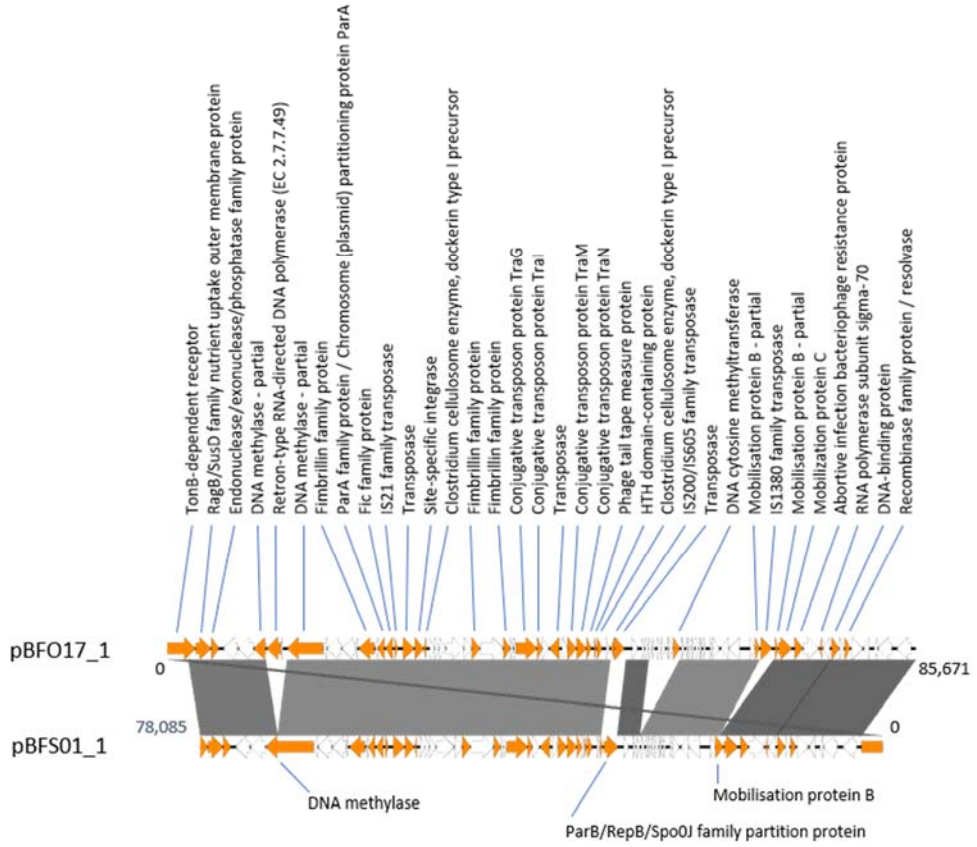

Figure 3. Linear representation of an alignment of putative circular plasmid sequences pBFO17_1 pBFS01_1. Comparison of the putative circular plasmids pBFO17_1 and pBFS01_1 (reverse complement for better visualisation) using EasyFig (82). EasyFig uses BLAST to identify sequences of similarity. Sequence similarities of >98% is indicated by full colouring, a darker colour indicates a higher %ID. Products of annotated CDS' are shown. CDS' annotated as hypothetical or Domain of Unknown Function are coloured white. The two sequences show a very high degree of similarity. pBFO17_1 is 7,586 bp longer than pBFS01_1. This is mainly due to the insertion of a reverse transcriptase (pBFO17_1, 11367..13034) (disrupting a DNA methylase), the insertion of prophage from position 56125 to 61162) (identified as an incomplete prophage using PHASTER (83)) and an IS*1380* family-like transposase (67933..69237). The regions pBFO17_1 50711..52501 and pBFS01_1 32248..30304 are not similar. Possibly, the insertion of two transposases in pBFO17_1 have excised most of the ParB-family DNA partitioning protein in the corresponding sequence range in pBFS01_1.

Antimicrobial susceptibility[a]				Antimicrobial resistance genes and IS elements[b]					
Strain	**Antimi-crobial**	**Etest MIC (mg/L)**	**Result**	**Gene**	**Upstream IS element**	**Sequence[c]**	**%ID**	**%COV**	**Associated resistance to drug class**
BFO17	MEM	>32	R	*cfiA11*	IS*614B*	Chr	100.00	99.20	Carbapenem
	IPM	>32	R						
	MTZ	>32	R	*nimJ*	IS*614B*	Chr	99.40	100.00	Nitroimidazole
				nimJ	IS*614B*	Chr_c	99.40	100.00	Nitroimidazole
	CLI	0.094	S						
	PTZ	>256	R						
				tetQ		Chr	99.34	99.34	Tetracycline
				cfxA4		Chr	85.71	100.00	Cephamycin
				bexB		Chr_c	91.21	100.00	Fluoroquinolone
				bexA		Chr	73.77	99.02	Fluoroquinolone
BFO18	MEM	>32	R	*cfiA2_1*	IS*Bf12*	Chr	100.00	100.00	Carbapenem
	IPM	16	R				100.00	100.00	
	MTZ	16	R	*nimD*	IS*1169*	2	99.19	100.00	Nitroimidazole
	CLI	6	R	*ermF*[d]	IS*4351*	Chr_c	99.83	72.03	Clindamycin
					IS*Bthe1*[d]	Chr_c	70.97	97.19	
				erm(F)[d]		Chr_c	99.58	29.71	
				lnu(AN2)		Chr_c	100.00	100.00	Clindamycin
	PTZ	>256	R						
				ugd		Chr	65.69	53.04	Polymyxin
				bexA		Chr_c	73.60	99.02	Fluoroquinolone
				bexB		Chr	91.14	100.00	Fluoroquinolone
				tet(Q)		Chr_c	99.79	100.00	Tetracycline
				mef(En2)		Chr_c	99.83	100.00	Macrolides
S01	MEM	>32	R	*cfiA13_1*	IS*1187*	Chr	99.20	100.00	Carbapenem
	IPM	16	R						
	MTZ	64	R	*nimE*	IS*Bf6*	3	100.00	100.00	Nitroimidazole
	CLI	>32	R	*erm(F)*	IS*1187*	Chr	99.50	100.00	Clindamycin
	PTZ	6	S						
				tetQ		Chr	90.02	99.95	Tetracycline
				tet(Q)		Chr_c	99.84	100.00	Tetracycline
				bexB		Chr_c	91.06	100.00	Fluoroquinolone
				bexA		Chr	74.03	98.80	Fluoroquinolone
BFO42	MEM	0.094	S						
	IPM	0.25	S						
	MTZ	8	R	*nimA*	IS*Bf13*	2	98.64	96.61	Nitroimidazole
	CLI	>256	R	*erm(F)*	IS*613*	Chr	99.50	100.00	Clindamycin
				lnu(AN2)		Chr	100.00	100.00	Clindamycin
	PTZ	0.38	S						

				ugd		Chr	70.38	31.45	
				cepA-49		Chr$_c$	100.00	100.00	Cephalosporin
				mef(En2)		Chr	99.83	100.00	Macrolide
				ugd		Chr	71.15	31.11	Polymyxin
				tetQ		Chr$_c$	100.00	100.00	Tetracycline
				bexB		Chr	99.12	100.00	Fluoroquinolone
				ere(D)		Chr	96.66	100.00	Erythromycin
				aadS		Chr$_c$	99.88	100.00	Aminoglycoside
				OXA-347	IS*613*	Chr$_c$	100.00	100.00	Penicillin, cephalosporin
				bexA		Chr	75.09	99.62	Fluoroquinolone
BFO67	MEM	8	R	*cfiA13_1*	None	Chr	100.00	100.00	Carbapenem
	IPM	0.5	S						
	MTZ	0.19	S						
	CLI	0.38	S						
	PTZ	2	S						
				cfxA2	IS*Bf11*	Chr	99.69	100.00	Cephamycin
				mef(En2)		Chr	99.75	100.00	Macrolide
				lnu(AN2)		Chr	100.00	100.00	Clindamycin
				ugd		Chr$_c$	66.76	56.30	Polymyxin
				tet(Q)		Chr	100.00	100.00	Tetracycline
				bexB		Chr$_c$	90.92	100.00	Fluoroquinolone
				bexA		Chr	73.90	99.02	Fluoroquinolone
BFO85	MEM	32	R	*cfiA2_1*	None	Chr	100.00	100.00	Carbapenem
	IPM	1	S						
	MTZ	0.25	S						
	CLI	>256	R	*ermB*		Chr$_c$	99.19	98.66	Clindamycin
	PTZ	2	S						
				ugd		Chr	69.84	31.45	Polymyxin
				tetQ		Chr$_c$	90.02	99.95	Tetracycline
				aadE		Chr$_c$	100.00	100.00	Aminoglycoside
				aad9		Chr$_c$	100.00	100.00	Aminoglycoside
				bexB		Chr$_c$	90.92	100.00	Fluoroquinolone
				bexA		Chr	73.53	99.02	Fluoroquinolone
				cfxA2	IS*614*	Chr$_c$	100.00	100.00	Cephamycin
				tet(Q)		Chr$_c$	99.84	100.00	Tetracycline

Table 5. Antimicrobial susceptibility and resistance genes and IS elements for the six MDR *B. fragilis* strains. Identified genes are displayed next to the relevant antimicrobials. Identified IS elements in correct orientation (opposite strand) directly upstream of the genes are included. The %ID and %COV refer to the gene hit. Hits with %ID or %COV <98% were confirmed with BLASTx searches. The hits for *ugd* represent possible homologs for genes coding for PmrE, which is involved in polymyxin resistance in Gram-negative bacteria. Full ABRicate results with nucleotide positions and information on the IS elements is available as Supplementary Tables S4 AMR-IS-results.xlsx. Notes: [a] Results from previously published work following EUCAST breakpoints (14). [c] A $_c$ denotes complement strand. [d] A transposase has inserted itself, splitting the *ermF* gene in two. Abbreviations: %ID; percent identity, %COV; coverage percentage, Chr; chromosome.

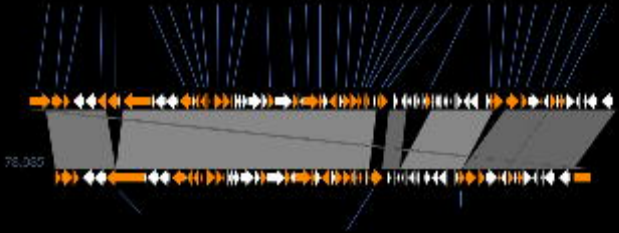
78,085

Strain	Best Spades graph	Hybrid assembly after first nanopore sequencing run. No Canu correction	Hybrid assembly after first nanopore sequencing run with Canu correction	Hybrid assembly with data from supplementary runs with Canu correction	After manual finishing	Final assemblies contig statistics		
						No.	Length	Relative read depth
CCUG 4856T	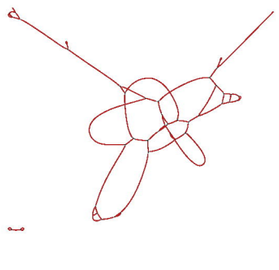	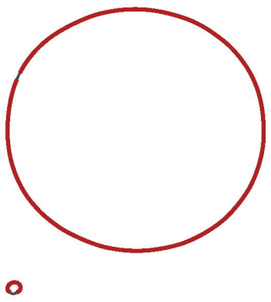	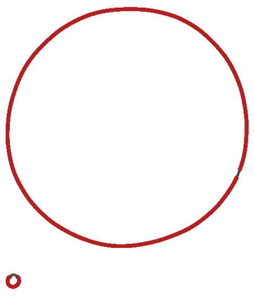	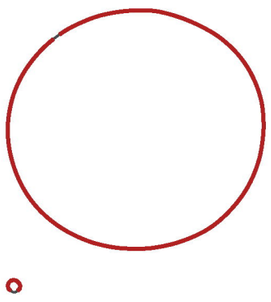		1 2	5,205,133 36,560	1.00x 7.42x
BFO17	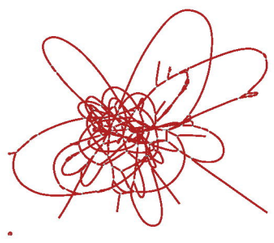	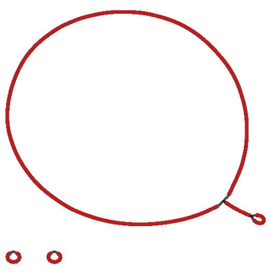	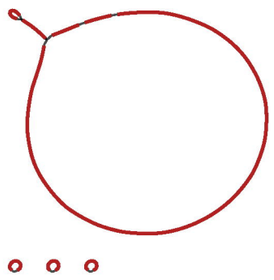	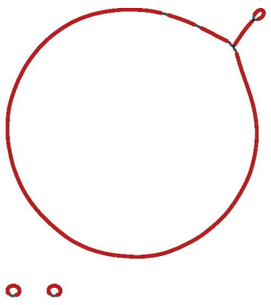	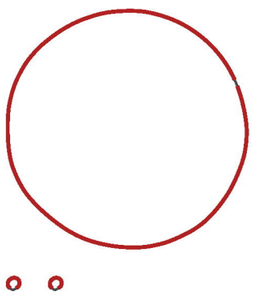	1 2 3	5,474,541 85,671 5,594	1.00x 1.85x 23.03x
BFO18		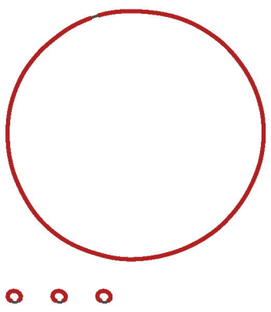	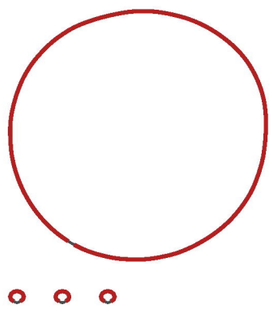	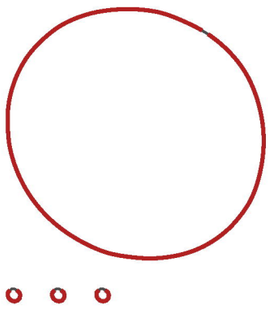		1 2 3 4	5,302,644 7,221 4,137 2,782	1.00x 25.98x 50.80x 59.91x
S01	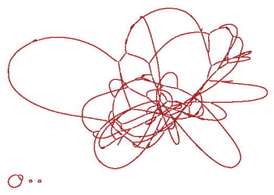	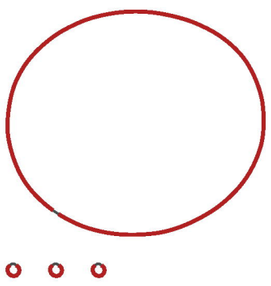	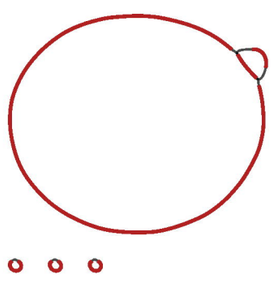	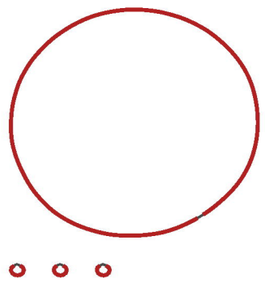		1 2 3 4	5,325,251 78,085 8,331 5,595	1.00x 2.29x 20.99x 22.67x
BFO42	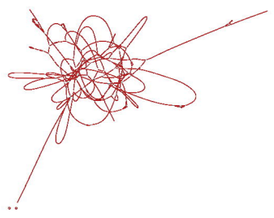	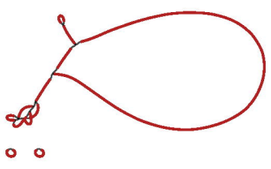	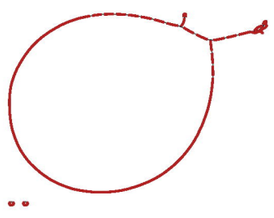	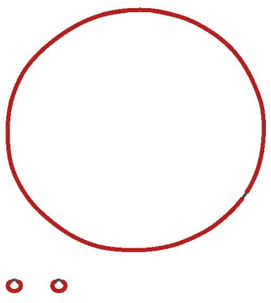		1 2 3	5,141,257 8,306 5,594	1.00x 40.06x 40.15x
BFO67	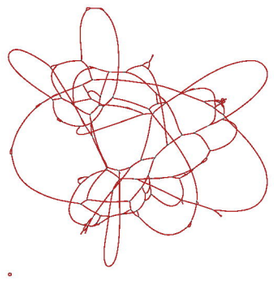	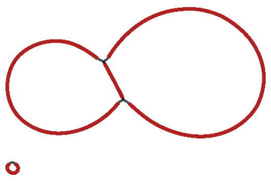	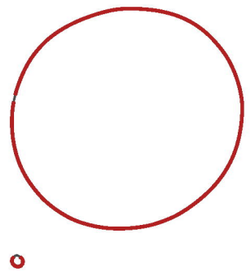	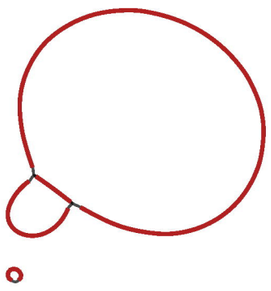	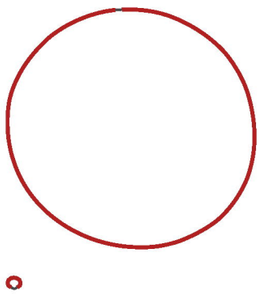	1 2	5,478,614 6,129	1.00x 94.15x
BFO85	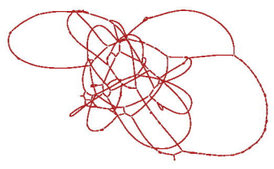	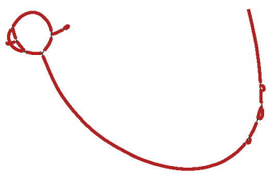	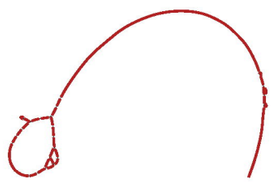	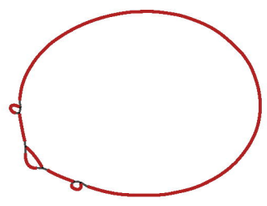	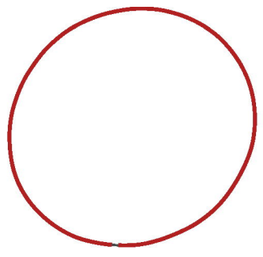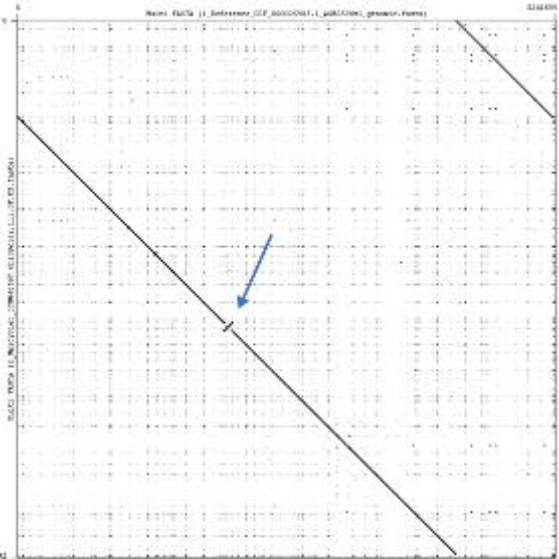	1	5,504,076	1.00x